

ROCK SLOPE STABILITY ASSESSMENT USING
PHOTOGRAMMETRIC MAPPING AND
LIMIT EQUILIBRIUM METHOD

TUNG WEN YAN

SCHOOL OF CIVIL ENGINEERING
UNIVERSITI SAINS MALAYSIA
2018

ROCK SLOPE STABILITY ASSESSMENT USING
PHOTOGRAMMETRIC MAPPING AND
LIMIT EQUILIBRIUM METHOD

By

TUNG WEN YAN

This dissertation is submitted to

UNIVERSITI SAINS MALAYSIA

As partial fulfillment of requirement for the degree of

**BACHELOR OF ENGINEERING (HONS.)
(CIVIL ENGINEERING)**

School of Civil Engineering
Universiti Sains Malaysia

June 2018



**SCHOOL OF CIVIL ENGINEERING
ACADEMIC SESSION 2017/2018
FINAL YEAR PROJECT EAA492/6
DISSERTATION ENDORSEMENT FORM**

Title: ROCK SLOPE STABILITY ASSESSMENT USING PHOTOGRAMMETRIC
MAPPING AND LIMIT EQUILIBRIUM METHOD

Name of Student: TUNG WEN YAN

I hereby declare that all corrections and comments made by the supervisor(s) and
examiner have been taken into consideration and rectified accordingly.

Signature:

Approved by:

(Signature of Supervisor)

Date :

Name of Supervisor :

Date :

Approved by:

(Signature of Examiner)

Name of Examiner:

Date :

ACKNOWLEDGEMENT

First and foremost, I would like to extend my heartfelt gratitude to my supervisor, Associate Professor Dr. Mohd Ashraf Mohamad Ismail from the School of Civil Engineering, Universiti Sains Malaysia for his continuous and tremendous supports of my research work, for his patience, motivation, encouragement, enthusiasm and immense knowledge. The door to his office was always open whenever I was overwhelmed with challenges or had a question about my research. His guidance helped me in all the time of research and writing of this thesis. I could not have imagined having a better advisor and mentor for my final year project.

Besides, I would like to express my sincere appreciation to the lecturers and technicians at School of Civil Engineering who are willing to lend me the equipment which was useful in my research work. This has contributed to the success of my research work.

Moreover, I would like to deliver my appreciation to my peers who have assisted me in the fieldwork data acquisition. Without their assistance and dedicated involvement throughout the process, the data collection would have never been accomplished. Not forgetting also to my peers who support and give valuable comments on my research work.

Finally, I must express my very profound gratitude to my parents for providing me with unfailing support and continuous encouragement throughout my years of study and through the process of researching and writing this thesis. This accomplishment would not have been possible without them. Thank you.

ABSTRAK

Penggalian cerun batu untuk pembangunan infrastruktur seperti lebuh raya dan saluran air tidak dapat dielakkan. Oleh itu, pencirian cerun batu dan tanggungan reka bentuk yang betul harus dilakukan untuk memastikan kestabilan cerun batu. Penggunaan teknik kajian garis imbasan dalam pengukuran orientasi ketakselajaran di cerun batu mengambil masa panjang dan amat mencabar disebabkan akses yang terhad. Struktur dari gerakan (SfM) yang menggunakan UAV merupakan satu cara yang cepat dan murah untuk melakukan pemetaan tinjauan tentang pencirian geoteknikal cerun batu berbanding dengan pengimbasan laser daratan (TLS). Gambar yang ditangkap dan diproses melalui pelarasan bundle dengan titikan kawalan tanah (GCP) dapat menghasilkan titik awan padat, model 3D, model digital permukaan (DSM) dan gambar ortho dengan ketepatan dalam lingkungan sentimeter. Satu kajian telah dilakukan di cerun batu di Projek Lencongan Banjir Barat Timah Tasoh, Perlis. Titik awan padat diimport ke dalam CloudCompare untuk mengekstrak data permukaan geologi. Data permukaan geologi tersebut adalah amat tepat kerana jurang dengan data diukur secara manual adalah dalam lingkungan 7° . Seterusnya, dengan menggunakan data ketakselajaran, analisis kinematik menunjukkan bahawa cerun batu mempunyai 15.40% risiko dalam slaid planar, 7.16% dalam slaid baji dan 1.33% dalam guling lenturan. Kestabilan cerun batu dianalisis dengan kaedah keseimbangan had (LEM) deterministik dalam 3D dan 2D serta LEM probabilistik dalam 2D. Geometri cerun batu, orientasi ketakselajaran dan parameter yang diperolehi daripada pangkalan data digunakan dalam analisis. Dengan kaedah deterministik, FoS diperolehi daripada 3D (0.908) adalah lebih tinggi daripada 2D (0.591). FoS probabilistik dalam 2D adalah

rendah (0.336) berbanding dengan deterministik (0.591). Kaedah probabilistik adalah lebih konservatif kerana mengambil kira ciri-ciri kepelbagaian dalam jisim batuan.

ABSTRACT

Rock slope excavation is unavoidable for the infrastructure development in our country such as expressway and water channel. Hence, a proper rock slope characterization and support design has to be carried out to ensure the stability of the rock slope, preventing hazardous events. Measuring discontinuity orientation in the rock slope by traditional scanline survey is time consuming and challenging due to the accessibility issue. Structure from motion (SfM) photogrammetry using UAV permits a fast and inexpensive way to do survey mapping for geotechnical characterization of rock slope compared to terrestrial laser scanner (TLS). Images that are captured and going through bundle adjustment with ground control points (GCPs) render within centimetre accuracy of dense point cloud, 3D model, orthophoto and digital surface model (DSM). A case study was conducted at the rock slope of Projek Lencongan Banjir Barat Timah Tasoh, Perlis. Dense point cloud is imported into CloudCompare to extract the geological planes. The discontinuities extracted are reliable and accurate as they are within 7° of the data measured manually. By using discontinuity data, the kinematic analysis shows that the rock slope has 15.40% of risk in planar sliding, 7.16% in wedge sliding and 1.33% in flexural toppling. Rock slope stability is analysed by deterministic Limit Equilibrium Method (LEM) in 3D and 2D and probabilistic LEM in 2D, utilising the 3D rock slope model geometry and orientation discontinuity extracted as well as the parameters obtained from the database. By comparing deterministic method, FoS obtained from 3D analysis (0.908) is higher than 2D analysis (0.591). On the other hand, by comparing probabilistic and deterministic method in 2D analysis, probabilistic method renders lower FoS (0.336) than deterministic method

(0.591). Probabilistic method is more conservative as it considers the heterogeneity characteristic of the rock mass.

TABLE OF CONTENTS

ACKNOWLEDGEMENT.....	ii
ABSTRAK	iii
ABSTRACT.....	v
TABLE OF CONTENTS	vii
LIST OF FIGURES	xi
LIST OF TABLES	xvii
LIST OF ABBREVIATIONS	xix
CHAPTER 1 INTRODUCTION.....	1
1.1 Background	1
1.2 Problem Statement	4
1.3 Objective	6
1.4 Scope of Work.....	7
1.5 Dissertation Outline	8
CHAPTER 2 LITERATURE REVIEW.....	10
2.1 Overview	10
2.2 SfM Photogrammetry	10
2.2.1 Reliability of SfM Photogrammetry	11
2.2.2 Application of SfM Photogrammetry	14
2.3 Real Time Kinematic (RTK).....	16
2.3.1 Accuracy of Real Time Kinematic (RTK).....	17
2.3.1.1 Factors Affecting Accuracy of Data Received from RTK.....	18
2.4 Extraction of Discontinuity	19
2.5 Generalised Hoek Brown Failure Criterion	20
2.6 Kinematic Analysis	22
2.7 Limit Equilibrium Method (LEM)	23
2.7.1 Morgensten-Price Analysis Method	25
2.7.2 Cuckoo Search Slip Surface Search Method	26
2.7.3 Probabilistic Method.....	27

CHAPTER 3 METHODOLOGY	29
3.1 Overview	29
3.2 Study Area.....	32
3.2.1 Slope in USM Main Campus	32
3.2.2 Rock Slope in Perlis.....	33
3.2.2.1 Geological Background	34
3.3 Slope Mapping – Fieldwork Data Acquisition.....	36
3.3.1 Design, Components and Specifications of UAV	37
3.3.2 Ground Control Point (GCP).....	39
3.3.3 Flight Path Planning and Photogrammetric Acquisition	42
3.4 Processing of Digital Photographs and Dataset	44
3.5 Extraction of Elevation Data.....	45
3.6 Rock Slope Discontinuity Orientation Acquisition.....	46
3.7 Extraction of Geological Planes.....	46
3.8 Rock Mass Properties.....	48
3.8.1 Uniaxial Compressive Strength (UCS) Test.....	48
3.8.2 Generalised Hoek-Brown Failure Criterion.....	50
3.8.2.1 Uniaxial Compressive Strength of Intact Rock (σ_{ci})	52
3.8.2.2 Mi Value	53
3.8.2.3 Geological Strength Index (GSI).....	54
3.8.2.4 Disturbance Factor (D)	55
3.9 Rock Slope Kinematic Analysis.....	56
3.9.1 Create a Stereonet	57
3.9.2 Add Set and Plane.....	59
3.9.3 Kinematic Analysis.....	59
3.9.4 Sensitivity Analysis	60
3.10 3D Limit Equilibrium Rock Slope Stability Analysis	61
3.10.1 Build Geometry Model	62
3.10.2 Limit Equilibrium Analysis Method.....	63
3.10.3 Define Rock Slope Material	66
3.10.3.1 Generalised Hoek-Brown Failure Criterion	66
3.10.3.2 Generalised Anisotropic Strength Model	67
3.10.3.3 Mohr Coulomb Failure Criterion.....	69
3.10.4 Assign Material.....	69
3.10.5 3D Slip Surface Search Method.....	70

3.10.6	Compute 3D Slope Stability Results	72
3.11	2D Limit Equilibrium Rock Slope Stability Analysis	73
3.11.1	Export Section Plane from 3D Geometry	73
3.11.2	Limit Equilibrium Analysis Method.....	74
3.11.3	Define Rock Slope Material	75
3.11.4	Assign Material.....	77
3.11.5	Probabilistic Analysis	77
3.11.6	2D Slip Surface Search Method.....	80
3.11.7	Compute 2D Slope Stability Result	81
CHAPTER 4 RESULTS AND DISCUSSION.....		82
4.1	Overview	82
4.2	Photogrammetric Data Analysis	84
4.2.1	Slope in USM Main Campus	84
4.2.1.1	Quantitative RMSE Accuracy Assessment	86
4.2.1.2	Qualitative Accuracy Assessment	92
4.2.2	Rock Slope in Perlis.....	94
4.2.2.1	Comparison of Bundle Adjustment with and without GCPs.....	98
4.3	Discontinuity Orientation of Rock Slope	101
4.3.1	Scanline Survey Method	102
4.3.2	Extraction of Geological Planes	103
4.3.3	Dip / Dip Direction Analysis	105
4.4	Rock Mass Properties.....	109
4.4.1	UCS Test Result.....	109
4.4.2	Rock Input Parameters.....	111
4.5	Rock Slope Kinematic Analysis.....	113
4.5.1	Planar Sliding.....	113
4.5.2	Wedge Sliding.....	114
4.5.3	Flexural Toppling	117
4.5.4	Sensitivity Analysis	118
4.6	Rock Slope Stability Analysis.....	122
CHAPTER 5 CONCLUSION AND RECOMMENDATIONS		129
5.1	Conclusion.....	129
5.2	Limitations	130
5.3	Recommendations	131

REFERENCES..... 132

APPENDIX A: UCS Test Results

LIST OF FIGURES

Figure 1.1: Structure of the thesis.....	9
Figure 2.1: Method of capturing images for photogrammetry (Ibraheem et al., 2014). 11	11
Figure 2.2: Real Time Kinematic (RTK) technique (Novatel Inc., 2015).....	17
Figure 3.1: Flow chart of research methodology.....	31
Figure 3.2: Slope in USM Main Campus.	32
Figure 3.3: Location of the slope in USM Main Campus (latitude, longitude: 5.361812, 100.308297) (Google Map, 2018) [2 nd February 2018].....	33
Figure 3.4: Rock slope in Perlis.....	33
Figure 3.5: Location of the rock slope in Perlis (latitude, longitude: 6.428794, 100.143884) (Google Map, 2018) [2 nd February 2018].	34
Figure 3.6: Geological map (stratigraphy) of Perlis and north of Kedah (Jones, 1981).35	35
Figure 3.7: Geological map (lithology) of Perlis and north of Kedah, Malaysia.	36
Figure 3.8: DJI Phantom 4 Pro Aircraft (DJI Phantom 4 Pro, 2016).	37
Figure 3.9: Location of RTK base stations in Malaysia (MyRTKnet, 2018)	40
Figure 3.10: RTK-GNSS Instrument - Leica Viva UNO CS10 controller with AS05 antenna set up on a GCP marker at Slope in USM.	41
Figure 3.11: Surveying at rock slope in Perlis (a) RTK-GNSS, (b) Total Station.	41
Figure 3.12: Flowchart of measuring coordinates of GCP by RTK-GNSS instrument. 41	41
Figure 3.13: Flight pathway for slope data acquisition in USM using UAV.	43
Figure 3.14: Flight pathway for rock slope data acquisition using UAV at (a) course angle 0°, (b) course angle 90°.....	43
Figure 3.15: Flowchart of processing images in Agisoft Photoscan Professional.....	45
Figure 3.16: Flowchart of extracting coordinates using Global Mapper software.	45

Figure 3.17: Geological compass.....	46
Figure 3.18: Flowchart of extraction of geological planes in CloudCompare using FACET plugin.....	47
Figure 3.19: (a) Rock coring machine, (b) Rock cutter trimmer.	49
Figure 3.20: Rock specimen with 50mm diameter and 100mm length.	49
Figure 3.21: Universal Testing Machine (UTM).....	50
Figure 3.22: Uniaxial Compressive Strength (UCS) of intact rock.	53
Figure 3.23: Mi value of rock type.	54
Figure 3.24: Geological Strength Index (GSI).....	55
Figure 3.25: Disturbance Factor (D).....	55
Figure 3.26: Slope failures and its stereonet (a) Planar Sliding, (b) Wedge sliding and (c) Flexural toppling (Hoek and Bray, 1981).....	56
Figure 3.27: Project settings.	58
Figure 3.28: Traverse information.	58
Figure 3.29: Stereonet plotted.....	58
Figure 3.30: Add user plane.....	59
Figure 3.31: Add set from cluster analysis.	59
Figure 3.32: Kinematic analysis.	60
Figure 3.33: Kinematic sensitivity analysis.....	60
Figure 3.34: 3D view of forces acting on a column (Huang et al., 2002).	62
Figure 3.35: Rock slope geometry imported into Rocscience Slide3.....	62
Figure 3.36: Create volume from rock slope surface geometry.	63
Figure 3.37: 3D rock slope stability analysis method.....	63
Figure 3.38: Forces acting on an infinitesimal slice (Morgenstern and Price, 1965). ...	64
Figure 3.39: Half-sine function.....	64

Figure 3.40: 3D slip surface discretized into square column (a) Top view, (b) View from YZ plane.	65
Figure 3.41: Inter-column data.	65
Figure 3.42: Define materials.	66
Figure 3.43: Rock mass parameters.	66
Figure 3.44: Angle of anisotropic plane.	67
Figure 3.45: Two anisotropic planes in the slope.	67
Figure 3.46: 2D representation of A and B angle parameters.	68
Figure 3.47: Graph of shear strength against the angle of anisotropy.	68
Figure 3.48: Anisotropic material parameters.	69
Figure 3.49: Assign material to the rock geometry.	69
Figure 3.50: Schematic diagram of Cuckoo Search algorithm.	70
Figure 3.51: 3D Slip surface options.	71
Figure 3.52: Computation of results.	72
Figure 3.53: Results output of 3D analysis.	72
Figure 3.54: Section export from Rocscience Slide3 to Slide.	73
Figure 3.55: 2D rock slope stability analysis method.	74
Figure 3.56: Slice data from Morgenstern-Price method.	74
Figure 3.57: Define materials.	75
Figure 3.58: Rock mass parameters – Generalised Hoek-Brown Failure Criterion.	75
Figure 3.59: Anisotropic Plane – Generalised Anisotropic Strength Model.	76
Figure 3.60: Angle of anisotropic plane.	76
Figure 3.61: Anisotropic material parameter – Mohr Coulomb Failure Criterion.	76
Figure 3.62: Assign material to the rock section plane.	77
Figure 3.63: Random variable samples used in probabilistic analysis.	78

Figure 3.64: Probabilistic analysis.....	79
Figure 3.65: Material statistics for probability analysis.	79
Figure 3.66: 2D slip surface option.	80
Figure 3.67: Computation of Results for 2D section of rock slope.	81
Figure 3.68: Results output from 2D analysis.	81
Figure 4.1: Location of markers at the slope in USM Main Campus.....	85
Figure 4.2: Aerial images of the slope in USM Main Campus captured using UAV. ..	86
Figure 4.3: Graph of average camera location errors for bundle adjustment without GCP at different flying heights.	87
Figure 4.4: Graph of RMSE of GCPs at different axis at various flying heights.	88
Figure 4.5: Graph of Total RMSE of GCPs at different flying heights.....	89
Figure 4.6: Graph of RMSE of GCPs with its CPs at various flying heights.....	90
Figure 4.7: Orthophoto of 80m flying height overlaid on Google Earth Pro (a) with GCP, (b) without GCP (Google Earth Pro, 2018) [2 nd February 2018].....	92
Figure 4.8: DSM of 80m flying height (a) with GCP, (b) without GCP.	93
Figure 4.9: Aerial images of the rock slope in Perlis captured using UAV.	94
Figure 4.10: Side images of the rock slope in Perlis captured using UAV.	94
Figure 4.11: Location of GCP markers at the rock slope in Perlis.	95
Figure 4.12: Dense point cloud of the rock slope (Top View).	96
Figure 4.13: 3D textured model of the rock slope (Top View).	97
Figure 4.14: Digital Surface Model (DSM) of the rock slope.	97
Figure 4.15: Contour generated at 5m interval.	97
Figure 4.16: Orthophoto with GCP overlays on Google Earth (Google Earth Pro, 2018) [20 th March 2018]	98
Figure 4.17: DSM of rock slope with six yellow lines as cross sections.....	99

Figure 4.18: Comparison of elevation between dataset without and with GCPs for (a) line 1, (b) line 2, (c) line 3, (d) line 4, (e) line 5 (f) and line 6.	100
Figure 4.19: Orientations were measured along the three lines.	103
Figure 4.20: Facets extracted from 3D dense cloud using FACET plugin in CloudCompare (a) Top view, (b) Front view.	104
Figure 4.21: Stereogram (a) Green set, (b) Blue set, (c) Entire rock slope.	104
Figure 4.22: Stereogram of orientations measured by scanline survey method.	106
Figure 4.23: Stereogram of orientations extracted from CloudCompare software.	106
Figure 4.24: Stereogram of all pole vectors extracted from CloudCompare software.	107
Figure 4.25: Rock Sample for UCS Testing (a) RQ1, (b) RQ2.	110
Figure 4.26: Rock specimen (a) before UCS test, (b) after UCS test.	110
Figure 4.27: Principal stress envelope of limestone.	112
Figure 4.28: Shear versus normal stress envelope of limestone.	112
Figure 4.29: Stereonet of planar sliding kinematic analysis.	114
Figure 4.30: Stereonet of wedge sliding kinematic analysis.	116
Figure 4.31: Stereonet of wedge sliding (with all plane intersections in blue).	116
Figure 4.32: Stereonet of flexural toppling kinematic analysis.	118
Figure 4.33: Kinematic sensitivity analysis for planar sliding failure mode.	119
Figure 4.34: Kinematic sensitivity analysis for wedge sliding failure mode.	120
Figure 4.35: Kinematic sensitivity analysis for flexural toppling failure mode.	121
Figure 4.36: FoS of rock slope without anisotropic plane in 3D. Cut section A is shown.	123
Figure 4.37: FoS of Cut Section A without anisotropic plane in 2D.	123
Figure 4.38: FoS of rock slope without anisotropic plane in 3D (control set). Cut Section B is shown.	124

Figure 4.39: FoS of Cut Section B with anisotropic plane in 2D.	124
Figure 4.40: FoS of rock slope with anisotropic plane in 3D.	
Cut section C is shown.....	126
Figure 4.41: FoS of Cut Section C with anisotropic plane in 2D.	126
Figure 4.42: FoS of rock slope with anisotropic plane in 3D.	
Cut section D is shown.	127
Figure 4.43: FoS of Cut Section D with anisotropic plane in 2D.	127

LIST OF TABLES

Table 2.1: Practical considerations of TLS and SfM photogrammetry for data acquisition (Wilkinson et al., 2016).....	13
Table 2.2: Design accuracy of RTK. (Department of Survey and Mapping Malaysia, 2005)	17
Table 2.3: Method of slices.....	24
Table 3.1: Specification of DJI Phantom 4 Pro (DJI Phantom 4 Pro, 2016).	38
Table 3.2: Guidelines for data acquisition using MyRTKnet (Department of Survey and Mapping Malaysia, 2005).....	40
Table 3.3: Details of flight mission at the slope in USM.	42
Table 3.4: Details of flight mission at the rock slope in Perlis.	43
Table 4.1: Number of images captured at various flying heights.....	85
Table 4.2: Coordinates of GCPs at the slope in USM Main Campus.....	85
Table 4.3: Coordinates of CPs at the slope in USM Main Campus.....	85
Table 4.4: Average camera location errors for bundle adjustment without GCP at different flying heights.....	86
Table 4.5: RMSE of GCPs for bundle adjustment with GCPs at different flying heights.....	87
Table 4.6: RMSE of CPs.....	89
Table 4.7: RMSE of check scale bar at different flying height	90
Table 4.8: Comparison of total RMSE with and without GCP at various flying heights.....	91
Table 4.9: DSM resolution of bundle adjustment with and without GCP.....	91
Table 4.10: Coordinates of GCPs for rock slope in Perlis.....	95

Table 4.11: Comparison of RMSE between bundle adjustment without and with GCPs.	99
Table 4.12: RMSE of control scale bars.	99
Table 4.13: Coordinates of cross-sections.	101
Table 4.14: Dip / dip direction obtained from scanline survey method.	102
Table 4.15: Comparison of dip / dip direction obtained manually and from software.	105
Table 4.16: Results of UCS of intact rock core specimens.	110
Table 4.17: Parameters of limestone rock slope	111
Table 4.18: Critical percentage of failure on different failure modes.	113
Table 4.19: FoS of with and without anisotropic plane in 3D and 2D analysis.	128

LIST OF ABBREVIATIONS

UAV	Unmanned Aerial Vehicle
UAS	Unmanned Aircraft System
SfM	Structure from Motion
TLS	Terrestrial Laser Scanner
RTK	Real Time Kinematic
GCP	Ground Control Point
CP	Check Point
GPS	Global Positioning System
GNSS	Global Navigation Satellite System
RTK	Real-Time Kinematic
CS	Cuckoo Search
RMSE	Root Mean Square Error
UTM	Universal Testing Machine
UCS	Uniaxial Compressive Strength
GSI	Geological Strength Index
D	Disturbance Factor
LEA	Limit Equilibrium Analysis
2D	Two Dimensional
3D	Three Dimensional
FoS	Factor of Safety
PF	Probability of Failure
RI	Reliability Index

CHAPTER 1

INTRODUCTION

1.1 Background

Malaysia is a mountainous country where almost half of it is over 150m above mean sea level and covered by granite, limestone, stratified rocks, igneous rocks, alluvium, etc. Nation's development involving building of infrastructure work such as expressway through the mountains is unavoidable as for the improvement of the connectivity and accessibility between one city and another. Hillside development has also increased for the past three decades in densely populated cities like Kuala Lumpur and Penang due to the limited flat and undulating lands in the cities. Nowadays, people would like to move to hilly area for the exclusivity, fresher air and better scenery (Gue and Wong, 2009). Besides, the excavation of rock slopes for irrigation and water channel is necessary to prevent flood occurrence in the area. Nonetheless, without proper design on the geotechnical aspect in the hilly terrain, it will be a hazard to the community. Moreover, geo-hazard incidents like rock slab detachment and rock falls might occur as a result of weathering processes and discontinuity factors characterized mainly by geological structure conditions such as jointing, fractures and day lighting of discontinuities. These geological hazards will affect the vulnerability of development in the encompassing areas. The impact of a rock fall can also affect its surrounding in which the air blast resulting from the fallen rock debris can be felt at a distance that is much further from the catastrophe area which could affect nearby buildings (Goh et al., 2017). Hence, it is crucial to carry out confirmatory geological slope mapping of the exposed slopes during construction of high cut slopes to detect any geological discontinuities that may cause potential failure mechanisms (Gue and Wong, 2009).

Rock mass is a high strength material if it is homogeneous and isotropic. Nevertheless, in reality, rock mass is heterogeneous and anisotropic since it has a lot of discontinuities and uncertainties due to the stresses induced by movement of tectonic plates and weathering effect. A discontinuity will manifest most commonly in a rock mass as a joint, fault, bedding surface, or blast damage. The orientations of the discontinuities contribute to the weakness in strength of the rock mass. Thus, it is vital to identify the discontinuity data in the rock slope.

There are many ways available to obtain the rock slope discontinuity data. Recently, the current advancement of new remote sensing strategies, such as Structure from Motion (SfM) photogrammetry and Terrestrial Laser Scanning (TLS) or LiDAR Scanning permit the obtaining of Earth surface datasets in a precise and fast way. SfM is a photogrammetric method for creating three-dimensional (3D) models of topography from multiple overlapping and stitching of two-dimensional (2D) photographs captured from multiple locations and orientations to reconstruct the photographed scene. In addition to ortho-rectified imagery, SfM produces a dense point cloud data set aligned with the coordinates obtained from Global Navigation Satellite System (GNSS) that is similar in many ways to that produced by TLS. Unlike high-resolution topographic surveying which is associated with high capital, SfM is an inexpensive, effective and flexible approach in capturing complex topography (Johnson et al., 2014). It is cost effective and ease of use compared to TLS. Decimate-scale vertical accuracy can be achieved using SfM even for sites with complex topography and a range of land-covers (Westoby et al., 2012). Unmanned aerial vehicle (UAV) with camera mounted on it is used to obtain photogrammetric data. The photogrammetry approach are used widely in geomorphological environments including river bed topography (Rusnák et al., 2018), glaciology (Dall'Asta et al., 2017;

Rossini et al., 2018), volcanology (Gomez and Kennedy, 2018), landslide (Gabrieli et al., 2016; Stumpf et al., 2015, 2014; Turner et al., 2015) and rock slope mapping for discontinuity characterization (Tannant, 2015). UAV images can produce slope map of the real site study area with highly accurate results (Tahar, 2015). With the output from the photogrammetric processes, the rock outcrop can be seen clearly with its geological planes. The data extraction from the geological planes is very important as it is one of the main inputs for the rock slope stability analysis.

In rock slope, plane sliding, wedge sliding and flexural toppling are common modes of failures due to the discontinuity in the rock mass. Plane mode of failure generally occurs in slice formed by stratified sedimentary and meta-sedimentary rock formations. The plane failure in rock slope occur when a structural discontinuity plane dips or daylight towards the valley at an angle smaller than the slope face angle and greater than the angle of friction of the discontinuity surface (Tang et al., 2017) . The strike of the potential discontinuity surface must be nearly parallel to the slope face. Tension crack must be present in the upper portion of the slope. Under such conditions the rock mass which rests on the discontinuity plane will slide down the slope when shearing stresses becomes more than the resisting forces (Hoek and Bray, 1981). Hence, by knowing the discontinuity orientations of the rock slope, the risk of rock failure in various modes can be determined.

There are two ways in analysing the rock slope stability: deterministic method and probabilistic method. Deterministic method uses the exact parameters input for analysis and only one output can be obtained. However, the probabilistic methods facilitate to incorporate parameters, which show uncertainty, in a systematic way and define the stability condition of the slope in probabilistic terms. For probabilistic analysis of a slope, having plane mode of failure, the parameters to be used are first

defined as fixed dimension parameters and as random variables (Hoek, 2007). Fixed dimension parameters are mainly the geometric parameters which can be obtained directly from the geometry of the slope such as; slope height, slope inclination, upper slope inclination and dip of the potential failure plane. The random variables are those which show uncertainty in their values and may vary considerably such as; cohesion and angle of friction, ratio of depth of water in tension crack to the depth of the tension crack etc. (Hoek, 2007). FoS is the ratio between the resisting forces and the driving forces. Since some of the parameters used in resisting and driving forces are random variables, the parameters will have probability distribution over certain range, rather than a fixed absolute value. Thus, the probabilistic analysis will also provide FoS as random variables with probability distribution (Raghuvanshi, 2017). In Monte-Carlo Simulation Approach, from the probability distribution of each variable, discrete values are randomly selected. Later, FoS is evaluated by utilizing a set of different discrete values of various parameters. Multiple simulations are made by repeating the process by taking different set of the discrete values of various variables (Zhao et al., 2016).

1.2 Problem Statement

The development of infrastructure work such as road and highway constructions involving deep cutting into the slope is unavoidable as it connects two cities with the shortest distance and traveling time. Besides, the need of development on hilly areas for building and residential purpose has also increased and these lead to the concern of safety and stability of the slope for the public. Hence, rock slope stability is concern about analyzing the structural fabric of the site to determine if the orientation of the discontinuities could result in instability of the slope under consideration. Nevertheless, in rock slopes, due to the structure of the cutting surface, rock mass typically exhibits

strong random properties, such as the structure of the surface geometry and mechanical parameters, resulting in a high degree of rock mass uncertainty. As a result, one of the greatest challenges for rock slope stability analysis is the selection of representative values from widely scattered discontinuity data. Hence, rock slope stability analysis using deterministic method is unsuitable. Deterministic analysis based on the factor of safety concept, requires a fixed representative value for each parameter without regard to the degree of uncertainty. Therefore, the deterministic analysis that is so common in engineering geology studies, fails to properly represent stochastic properties of discontinuities.

Generally, rock masses are heterogeneous and unpredictable as they contain discontinuities such as orientation, size, aperture, surface conditions (roughness and alteration), and frequency. Discontinuity plays an important role in the strength, stability, deformability and permeability of the rock mass. Besides, the soil material in the anisotropic plane will weaken the rock mass as well. Thus, the description of discontinuities in rock mass must be accurate to enhance the quality of geological input data for an effective geotechnical assessment. The ability of overcoming bias as well as the amount of data collected will have an effect on the discontinuity spacing and trace length measurements (Priest and Hudson, 1981). Traditional ways of characterizing the rock slope such as scanline survey, cell mapping and rapid face mapping which use a compass, an inclinometer and a measuring tape, have several disadvantages because rock mass exposures often have limited accessibility which affects the choice of sampling location. As a result, the site investigation is bias, hazardous, time consuming and expensive (Torres, 2008).

TLS and SfM photogrammetry are the current technologies available for topography mapping to produce rock slope geometry. However, the cost of acquisition

of TLS is expensive. Furthermore, many researches using TLS have been done and showed that the results are coherent with the results obtained from the traditional methods. However, there is less research on using UAV for rock slope mapping by SfM method. Thus, SfM photogrammetry using unmanned Aerial Vehicle (UAV), an alternative method to produce 3D dense point clouds will be carried out.

1.3 Objective

The objectives of this study are:

1. To determine the accuracy of using photogrammetry approach for slope mapping with and without ground control points (GCPs).
2. To determine the rock slope geometry and its geological structure using photogrammetry approach with the bundle adjustment of GCPs.
3. To verify the rock slope discontinuities orientations extracted digitally by the least square fitting algorithm in FACET plugin in CloudCompare with the data measured manually using scanline survey method.
4. To access the factor of safety (FoS) of the rock slope based on various discontinuities pattern using deterministic Limit Equilibrium Method (LEM) in 3D and 2D analysis and probabilistic LEM in 2D analysis.

1.4 Scope of Work

The scope of work is focusing on the accuracy assessment of photogrammetry approach processed with and without Ground Control Points (GCPs) by mapping a gentle slope at various flying heights. A quad copter (UAV) is used to capture the images of the slope. The dataset is processed with and without GCP where the GCP coordinates are obtained from Real-Time Kinematic Global Navigation Satellite System (RTK-GNSS) instrument. Then, a rock slope is mapped by following the same procedure as mapping the gentle slope at an optimum flying height. The photogrammetric data are processed with GCP to obtain the rock slope geometry and geological structure. The dip / dip direction of the discontinuity present in the rock slope is extracted digitally. Kinematic analysis is conducted using the orientation data to determine the critical percentage of planar sliding, wedge sliding and flexural toppling failure mode. Besides, rock slope stability analysis using limit equilibrium method is conducted to determine the critical safety factor of the rock slope by inputting the orientations extracted as the anisotropic plane and the rock mass parameters obtained from a database. Deterministic method with slip surface analyzing method, cuckoo search is carried out on the 3D rock slope. Then, by identifying the global minimum slip surface of the rock slope geometry in 3D, the critical cut section is extracted to analyse in 2D. Since the rock mass has uncertainty and variability, probabilistic method is used to analyse the 2D cut section. The scope of work is to achieve the main objectives of this research.

1.5 Dissertation Outline

This thesis consists of five chapters. Chapter 1 is the Introduction where this chapter provides an overview of the thesis, the problem statement, followed by the objectives of this research and the scope of work of this research. Chapter 2 is the Literature Review. This chapter provides critical theoretical and conceptual understanding about the research. The previous works conducted by other researchers serve as basic knowledge for the study. Next is chapter 3: Methodology. This chapter discusses the study area and comprehensive descriptions on the overall methods that have been applied in this study. The flow will be viewed in detail to facilitate the understanding on the execution of the research. Chapter 4 is about results and discussion. This chapter involves data processing, analysis, interpretation and evaluation of the rock slope stability by using software application. Lastly, chapter 5 is Conclusion. This chapter summarizes and concludes the findings in this research. All the limitations of the study and assumption that have made throughout the study are listed. Some suggestions and recommendations for further study of this topic are clearly listed in this chapter. The overview structure of the thesis is depicted in Figure 1.1.

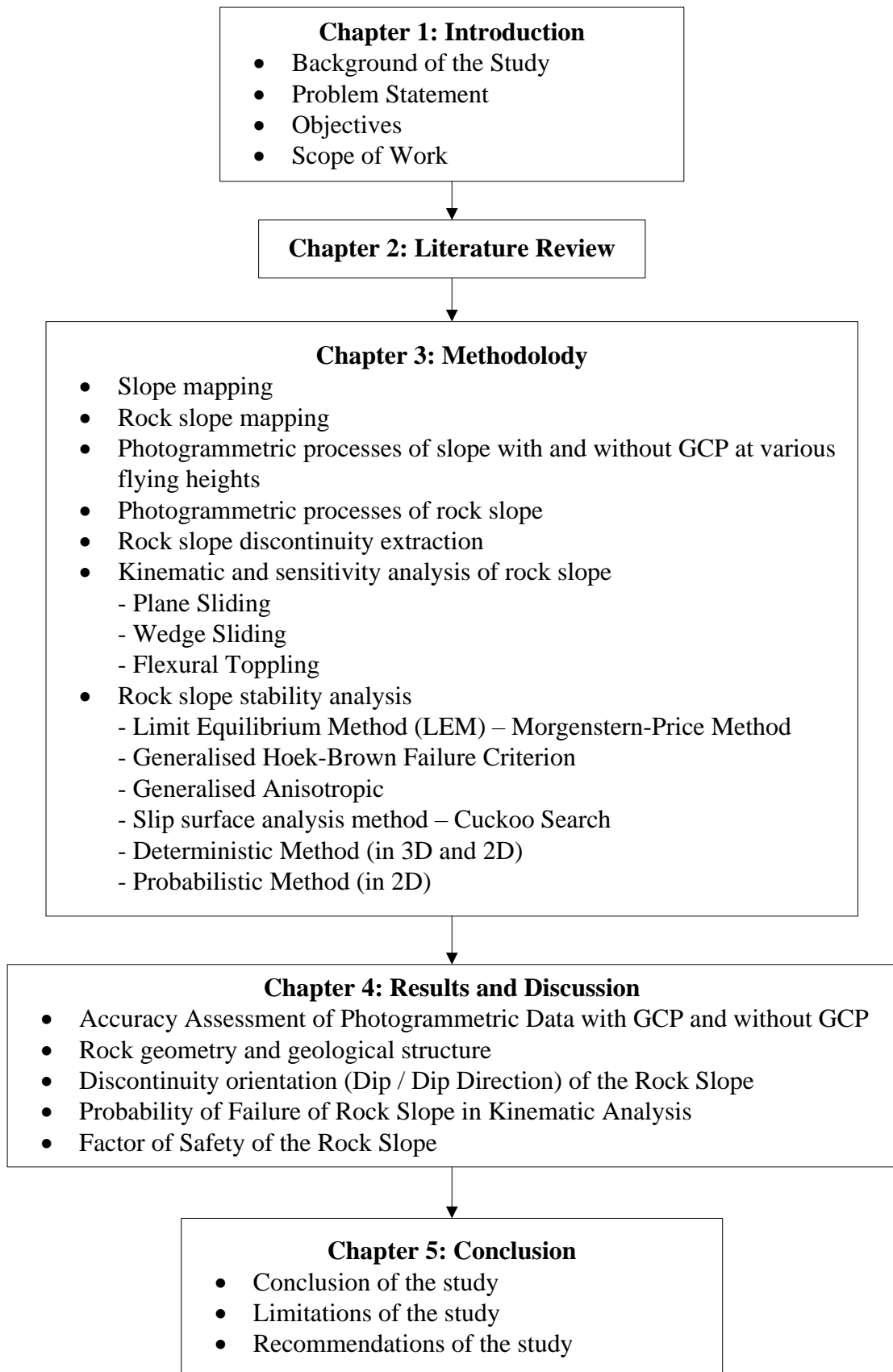


Figure 1.1: Structure of the thesis.

CHAPTER 2

LITERATURE REVIEW

2.1 Overview

Literature review is predominant for any research. It includes the previous work conducted by other researchers. This chapter reviews the application of Structure from Motion (SfM) photogrammetry and its accuracy on the research work. The accuracy of the technique of getting the exact location, Real Time Kinematic (RTK) is discussed. Besides, this chapter also discusses the previous work on extracting discontinuity of rock mass automatically. Moreover, the rock slope stability analysis method is discussed.

2.2 SfM Photogrammetry

Photogrammetry is a measurement technique that uses light rays captured by a camera. Structure from Motion (SfM) is an image processing technique that was originally developed for computer vision applications. Some fundamental mathematics used in SfM techniques, including camera pose estimation, camera calibration, triangulation, and bundle adjustment, were adapted from photogrammetry. Using multiple overlapping images as shown in Figure 2.1, the SfM algorithms can estimate the camera pose parameters and generate sparse point-clouds. Further image processing using multiple view stereo can generate a dense point cloud once the correspondence among multiple camera locations has been established (Tannant, 2015). Image processing using SfM has been implemented in commercial software such as Agisoft Photoscan Professional. Unmanned aerial vehicle (UAV) can be considered as a low-cost alternative to the classical manned aerial photogrammetry. UAV, capable of

performing the photogrammetric data acquisition by capturing images with digital cameras, can fly in manual, semi-automated, and autonomous modes. Following a typical photogrammetric workflow, 3D results like digital surface or terrain models, contours, textured 3D models, vector information, etc. can be produced, even on large areas (Nex and Remondino, 2013). Agüera-Vega et al. (2018) claims that the development of UAV photogrammetry over the last decade has allowed terrain that is challenging for humans to access to be captured at very high spatial and temporal resolutions. UAV images can produce slope map of the real site study area with highly accurate results (Tahar, 2015).

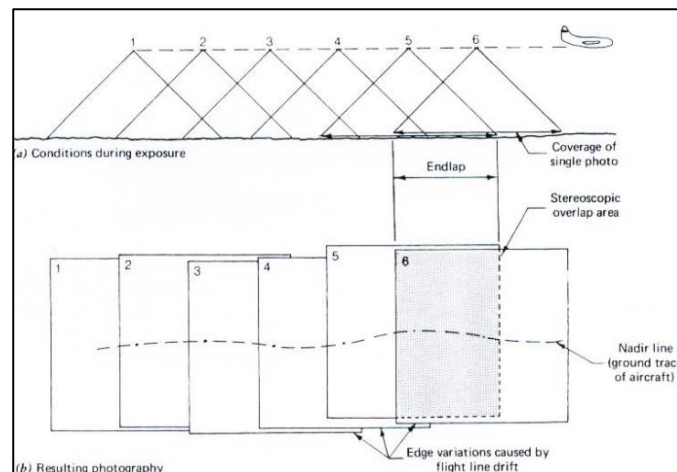


Figure 2.1: Method of capturing images for photogrammetry (Ibraheem et al., 2014).

2.2.1 Reliability of SfM Photogrammetry

Martin et al. (2007) has conducted a research on the comparison of the accuracy of the three-dimensional digital models of a 55m high rock slope derived from the ground-based LiDAR and digital photogrammetry survey. Canon 5D digital Single Lens Reflex camera with a 35mm Canon fixed focus lens with focus set at infinity and f/8 aperture was used to capture the images of the rock slope for photogrammetry. They

concluded that both survey methods gave similar DEM results that would be suitable for rock engineering problems as well as for extracting the orientation data of geological features. The overall error for LiDAR model is 138mm whereas for photogrammetry model is 98mm. This indicates photogrammetry approach renders good quality results. Although the density of the point cloud from LiDAR survey is denser which means smaller features could be extracted, it is not considered to be a practical advantage. The photogrammetry survey is quicker to conduct in the field compared to the LiDAR survey.

Another research was conducted by Wilkinson et al. (2016) on the comparison between the usage of TLS and SfM photogrammetry for the ground-based digital outcrop. The study was conducted on the outcrops from North East England and the United Arab Emirates. A 12 megapixel Nikon D300 with Nikon AF-S DX Nikkor 10–24 mm f/3.5–4.5G ED and Nikon AF-S DX Nikkor 55–200 mm f/4.5–5.6G IF-ED VR lenses camera were used for SfM. They claimed that both TLS and SfM are viable methods for use in the field, although no single technology is universally best suited to all situations. Table 2.1 shows the practical considerations and operating conditions of TLS and SfM where each method has clear advantages. The suitability of each method depends on the aim of the work, the expected outcome, the nature of the outcrop, and the prevalent operating conditions. Compared to LiDAR point clouds, RMSE of the photogram metric point clouds generally did not exceed 0.2m for the reconstruction of the entire landslide and 0.06 m for the reconstruction of the main scarp. The SfM technique currently remains less precise than TLS but provides spatially distributed information at significant lower costs and is, therefore, valuable for many practical landslide investigations (Stumpf et al., 2015).

Table 2.1: Practical considerations of TLS and SfM photogrammetry for data acquisition (Wilkinson et al., 2016).

	Terrestrial Laser Scanner (TLS)	Structure from Motion (SfM) photogrammetry
Typical Cost	High (\$50k – \$200k)	Low (\$650 – \$10k)
Weight	High (15 – 50kg)	Low (2 – 15kg)
Package size for transport	Large (small suitcase sized)	Small (daypack sized)
Number of operators	1+	1+
Level of operator training	Moderate	Moderate – high
Certainty of success (for critical application)²	High (results available immediately)	Moderate (final results known after images processed)
Immediate results in the field	Yes	No
Acquisition time	Comparable with SfM	Comparable with TLS
Precision	High (2 – 8mm, mostly independent of range)	Ultra high to ultra-low (image resolution and range dependent)
Accuracy	≈ 5cm (GPS dependent)	≈ 5cm (GPS dependent)
Detail (point spacing)	Low – high (range dependent)	Low – high (range dependent)
Internal consistency	High	Moderate
Processing time	Low (minutes to hours)	High (hours to days, dependent on workstation and desired detail)
Additional data	Laser reflection intensity per point	Normal to outcrop surface per point
Versatility in a range of applications³	High	Moderate (dependent on operator experience)
Ability to resume survey at a later time	High	Moderate (dependent on similar outcrop appearance)
Multi-day survey, without mains power	Moderate (extra batteries relatively expensive, bulky, and heavy)	High (extra batteries relatively cheap, small and light)
Remote operation for temporal survey	Yes	No; operator driven
Automated acquisition⁴	Yes	No; operator driven
Dependence on data from other sources	Low (GNSS provides orientation and location)	Moderate (GNSS provides scale, orientation, and location)
Depreciation of equipment value	Low	Low–moderate
Ruggedness	Moderate	Moderate
General availability	Low	Moderate–high
Ease of service and availability of replacement parts⁵	Low–moderate	Moderate–high
Equipment used in fieldwork for other purposes?	No	Yes
Ease of transport, import and/or export	Low - moderate	High

¹For the acquisition of data for rigorous quantitative analysis.
²The ability of the operator to review the acquired data in 3D before leaving the field.
³To consistently provide quality data for rigorous quantitative analysis.
⁴A measure of how much free time an operator has during the survey for other tasks, such as sample collection.
⁵TLS equipment must usually be returned to the manufacturer for servicing or part replacement by a specialist. SfM uses widely available camera equipment that can be serviced or replaced worldwide.
Note: GNSS—Global Navigation Satellite System.

Mapping fault zone topography in areas of sparse or low-lying vegetation using SfM and LiDAR was conducted. At 0.1km² alluvial fan on the San Andreas Fault, the closest point vertical distances of SfM (point cloud density > 700 points/m²) to LiDAR (much sparser point cloud density, 4 points/m²) is less than three centimeter. On the other hand, at 1km section of the 1992 Landers earthquake scarp, the closest point vertical distances of SfM to LiDAR is less than six centimeter. This concludes that SfM greatly facilitates the imaging of subtle geomorphic offsets related to past earthquakes as well as rapid response mapping or long-term monitoring of faulted landscapes (Johnson et al., 2014). In short, SfM photogrammetry can produce a good quality and high accuracy of photogrammetric outputs which is comparable to TLS.

2.2.2 Application of SfM Photogrammetry

Photogrammetry has been widely used for more than a century for different purposes. Its surveys are being increasingly used to collect high resolution airborne imagery in a wide variety of environmental and geomorphological environments.

Uysal et al. (2015) has conducted a research on using UAV to map a five hectare area. Accuracy of the Digital Elevation Model (DEM) was evaluated with 30 check points and obtained 6.62 cm overall vertical accuracy from an altitude of 60 m. This concludes that it is possible to use the SfM Photogrammetry data as map producing, surveying, and some other engineering applications with the advantages of low-cost, time conservation, and minimum field work. The SfM technique can also be applied in glaciology. An accuracy of 17cm was achieved for the generation of DSM and orthophoto of glacial morphology from SfM techniques (Rossini et al., 2018). Dall'Asta et al. (2017) also discovered that the RMSE differences found on twelve Check Points were about 4 cm in horizontal and 7 cm in elevation. Agüera-Vega et al.

(2018) utilizes the SfM photogrammetry in topography mapping. They collected two different image datasets by tilting the camera horizontally and at 45°. The best accuracies achieved were RMSE equal to 0.053 m, 0.070 m and 0.061 m in X, Y and Z direction respectively. Turner et al. (2015) uses UAV to collect a time series of high-resolution images over four years at seven epochs to assess landslide dynamics. The SfM photogrammetry applied create DSM of the landslide surface with an accuracy of 4-5cm in the horizontal and 3-4cm in the vertical direction. Besides, landslide study using SfM was also conducted by Carvajal et al. (2012). Md4-200 micro drones with an on-board calibrated camera 12 Megapixels Pentax Optio A40 was used in the study. The accuracy of the products is 0.049m for planimetric errors and 0.108m for altimetric errors. Tannant (2015) utilises SfM in steep rock slope mapping. The theoretical coordinate accuracy in the model was approximately 20 mm. This is more than adequate to characterize many geometric features of relevance to the wedge failure, which had a height and width of roughly 15m. Besides, the application of SfM photogrammetry was conducted in various fields such as landslide (Gabrieli et al., 2016; Niethammer et al., 2010; Peterman, 2015; Stumpf et al., 2015, 2014), rock slope mapping (Riquelme et al., 2017), river bed topography (Rusnák et al., 2018) and volcanology (Gomez and Kennedy, 2018).

From the previous studies, SfM photogrammetry can render a promising quality and accuracy of outputs. However, the accuracy of the resulting 3D coordinates of features on the ground is controlled by the choice of the resolutions of the camera, focal length of the lens, image overlapping ratio, flying altitude, usage of ground control points (GCP) and the coordinates data collected from GNSS instrument to geo-reference the images. Mesas-Carrascosa et al. (2016) discovered that higher image overlapping ratio will render lower RMSE errors. However, extremely high image

overlapping ratio will produce large image datasets, causing longer processing time. It is often helpful to avoid collection of too many photos as it is difficult to process and store (Tannant, 2015). Therefore, optimum images overlapping ratio is set based on the site mapping condition. In this study, DJI Phantom 4 Pro, a brand new UAV mounted with a 20 megapixel camera is used to study the effect of flying height to the RMSE errors as well as the bundle adjustment of images with the usage of GCP and without GCP.

2.3 Real Time Kinematic (RTK)

Real Time Kinematic (RTK) is a technique used to receive GNSS signals at a stationary reference with known position coordinates and to use these to correct position data at a roving receiver in another location which increases the accuracy of signal received as depicted in Figure 2.2. Real Time Kinematic has become a popular high precision technique in Malaysia. The Malaysian Real-Time Kinematic Network (MyRTKnet) has been developed to facilitate RTK positioning in Malaysia. MyRTKnet consists 78 reference stations located at Peninsular Malaysia, Sabah and Sarawak (Jamil et al., 2010). Virtual Reference System (VRS) is one of the services provided by MyRTKnet. It is an integrated system which links and utilizes data from permanent reference stations to model errors throughout the coverage area. This model is used to synthesize virtual reference stations near the user's location which then provide a localized set of standard format correction messages to the roving receiver (Department of Survey and Mapping Malaysia, 2005).

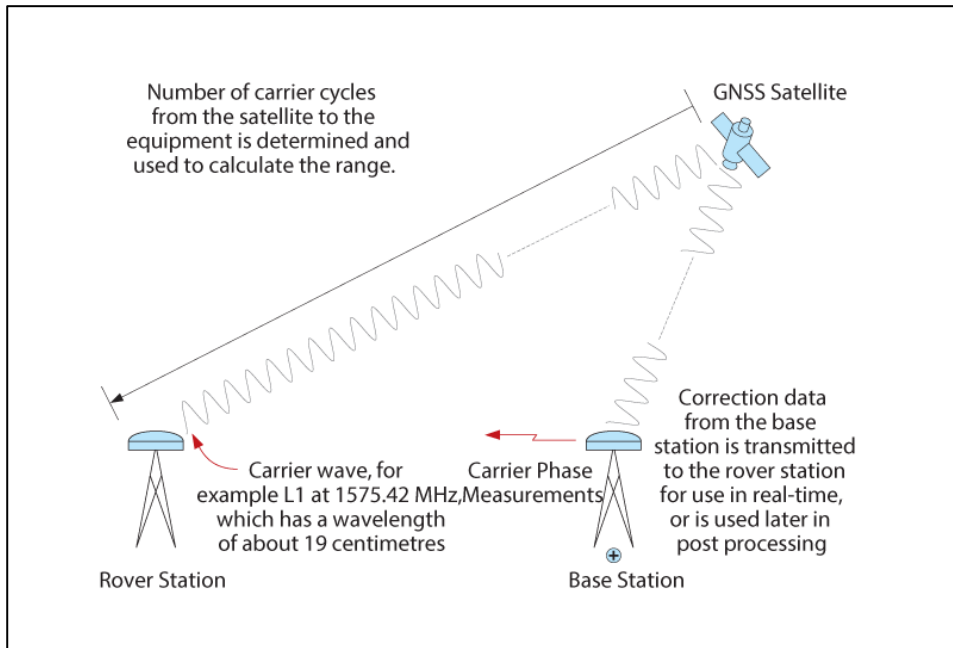


Figure 2.2: Real Time Kinematic (RTK) technique (Novatel Inc., 2015).

2.3.1 Accuracy of Real Time Kinematic (RTK)

The design accuracy of the minimum performance anticipated from MyRTKnet real-time services is outlined in Table 2.2. It would be evident from the table that centimeter level accuracy would be achievable where Virtual Reference System (VRS) services are available. Additionally, such level of accuracy could also be achieved within 30 km off MyRTKnet reference stations.

Table 2.2: Design accuracy of RTK (Department of Survey and Mapping Malaysia, 2005).

Operation Mode (Instrumentation)	Design Real-Time Accuracy @ 95% Confidence Level (single-point positioning mode)	
	Horizontal	Vertical
VRS	4 cm	6 cm
Single Base	4 cm	6 cm
Network DGPS	0.3 m	0.6 m

A study on practical accuracy of the RTK positioning using VRS generated by MyRTKnet outside the network was conducted by Sulaiman et al. (2009). A conclusion can be made that the accuracy achieved was up to 6cm in horizontal component and up to 8cm in vertical component although the distance of data acquisition was 30km away from the nearest physical reference station. Similar research was conducted and the results show that the accuracies in the horizontal and height component were less than 1 cm and 9 cm respectively. It also shows that for areas within 30 km from the network, the accuracies obtained were within the said levels (Jamil et al., 2010). Saghravani and Saghravani (2009) discovered the vertical accuracy achieved by RTK-GPS is within 10cm. The overall reliability of RTK-GPS in case of elevation is more than 95%.

2.3.1.1 Factors Affecting Accuracy of Data Received from RTK

The accuracy of the data acquisition is not solely depended on the VRS network provided by the MyRTKnet. The overall performance will be dependent on uninterrupted data communication and GPS system characteristics, including data transmission latency, ionospheric activity, tropospheric activity, satellite geometry, baseline length, multipath effects and user instrumentation. Multipath error is a positioning error resulting from interference between radio waves which have travelled between the transmitter and the receiver by two paths of different electrical lengths. Data latency is the time taken for the user to send his approximate position to the GPS net server and receive back correction in order to initialize positioning. As tested by Department of Survey and Mapping Malaysia (2005), the average initialization time was 20 seconds. The common factors affecting time to initialize are rover station satellites geometry and sky clearance. Different RTK-GNSS instrument will render different quality of results based on its specifications and settings. The baseline

precision of a differential code solution for static and kinematic surveys is 40 cm (Leica Geosystems, 2012). This indicates that the instrument used must be compatible to receive a high accuracy data so that data less than 10cm error can be obtained. For higher accuracies, users may opt for post-processing approach, by obtaining the MyRTKnet data files in Receiver Independent Exchange format (RINEX format) which are stored and managed separately by Geodesy Section of JUPEM (Department of Survey and Mapping Malaysia, 2005). However, the time taken for this static method is longer compared to RTK.

2.4 Extraction of Discontinuity

The description of geological structures from rock exposures is traditionally achieved using a compass, an inclinometer, and a measuring tape. The data are recorded on a notebook and the rock faces are then photographed with a camera for documentation purposes. However, this method, known as the scanline mapping method, has several drawbacks. It cannot be applied to physically inaccessible or unsafe areas and unsupported underground mining areas. Most often, the rock mass exposures have either limited accessibility or complete inaccessibility, thus making field investigations time consuming, expensive, and hazardous. Furthermore, it only provides a linear sampling of a two-dimensional domain, resulting in important biases in the collected datasets. The ability of overcoming bias as well as the amount of data collected will have an effect on the discontinuity spacing and trace length measurements (Priest and Hudson, 1981). Planes in the rock outcrops depict a lot of useful information such as tectonic history, rock mass strength, sediment processes, etc. Hence, surface mapping techniques such as photogrammetry which can produce dense point clouds can overcome these practical difficulties as it can record the entire

discontinuities of the rock slope. Nevertheless, with the dense cloud, algorithm must be invented to extract the planes and discontinuities quantitatively so that it is useful for geotechnical designing work. A study was conducted to identify the discontinuity sets semi-automatically with Discontinuity Set Extractor (DSE) software and calculate the spacing of the sets (Buyer and Schubert, 2017). Also, a number of researchers have developed their own algorithms in different environments to extract the discontinuity. (Buyer and Schubert, 2016; Chen et al., 2016; Chen et al., 2017; Guo et al., 2017; Lato and Vöge, 2012; Riquelme et al., 2014). However, the algorithm process is complicated and can hardly obtain. Dewez et al. (2016) created an automated geological plane extraction plugin named FACETS that is dedicated within CloudCompare software by applying least square fitting algorithm. The procedures are friendly user and can export quantitative discontinuity orientation (dip/dip direction). The case study has proven that the FACETS plugin can extract the geological planes accurately within 10° of difference compared to scanline survey method. However, only one research was done using the plugin. Thus, the plugin is used to extract the discontinuity of the rock mass in this research work and will be verified by the manual scanline survey method. The technique used allows for systematic mapping and the building of a permanent and huge database for rock mass characterization.

2.5 Generalised Hoek Brown Failure Criterion

The Hoek–Brown failure criterion (Hoek and Brown, 1980) is an empirical stress surface that is used in rock mechanics to predict the failure of rock. The Hoek–Brown failure criterion is an empirically derived relationship used to describe a non-linear increase in peak strength of isotropic rock with increasing confining stress. Hoek–Brown follows a non-linear, parabolic form that distinguishes it from the linear

Mohr–Coulomb failure criterion. The criterion includes companion procedures developed to provide a practical means to estimate rock mass strength from laboratory test values and field observations.

At first, the criterion was introduced in an attempt to provide input data for the analyses required for the design of underground excavations in hard rock. However, due to the lack of suitable alternatives, the criterion was soon adopted by the rock mechanics community and its use quickly spread beyond the original limits used in deriving the strength reduction relationships. Consequently, it has to be examined and improved from time to time to account for the wide range of practical problems to which the criterion was being applied. Generalised Hoek Brown Failure Criterion was introduced (Hoek et al., 2002). Since most geotechnical software is still written in terms of the Mohr-Coulomb failure criterion, it is necessary to determine equivalent angles of friction and cohesive strengths for each rock mass and stress. The relationship between major and minor principal stresses of Generalised Hoek-Brown and equivalent Mohr-Coulomb criteria is discovered. The significant contribution to this criterion was that it linked the equation to geological observations, initially to Bieniawski Rock Mass Rating and later to the Geological Strength Index (GSI) (Hoek and Brown, 1997). Besides, the disturbance factor was added to become a factor in determining the strength of the rock mass. The level of disturbance can be particularly significant when the slope is formed using blasting techniques. A rigorous set of analyses have been performed where the level of disturbance is considered as constant or linearly varying throughout the slope. The disturbance factor was found to have significant influence on the rock slope stability assessment, especially for poorer quality rock masses (Li et al., 2011). In addition, utilising stability charts to estimate the stability of cut rock slopes without considering the rock mass disturbance may lead to significant overestimations.

(Li and Wu, 2013) states that with the increase of D , the FoS of slope decreases linearly; as GSI increases, FoS increases non-linearly. When σ_{ci} is small, FoS and σ_{ci} shows certain nonlinear characteristic, when σ_{ci} is large, they show linear relationship characteristics. As m_i increases, FoS decreases first and then increases. Mohammadi and Tavakoli (2015) have investigated the applicability of generalized Hoek-Brown and Mohr-Coulomb failure criteria for determining the stresses on failure plane of rock. Results show that the obtained stresses and angles of failure plane for GHB results are closer to the empirical results. Moreover, the failure criterion is applied by Dong-ping et al. (2016) and Pan et al. (2017).

2.6 Kinematic Analysis

Kinematics refers to the motion of bodies without reference to the forces that cause them to move. Many rock cuts are stable on steep slopes even though they contain steeply inclined planes of weakness with exceedingly low strength; this happens when there is no freedom for a block to move along the weak surface because other ledges of intact rock are in the way. Should the blockage be removed by erosion, excavation, or growth of cracks, the slope would fail immediately Kinematic analysis is often used to investigate and determine the probability of structurally controlled failures such as planar sliding, wedge sliding, and toppling (Goodman, 1989). For rock slopes containing discontinuities, the uncertainty and variability in rock slope, generally arises from dominating joints and slope face azimuth and the discontinuity strength. Kinematic analysis is analysed mainly using the directionality of the discontinuous rock mass. The discontinuity orientations of the rock slope are projected onto a stereonet for the analysis. Case studies of rock slopes have been conducted by the researchers using kinematic analysis (Goh et al., 2017; Greif and Vlcko, 2017; Margottini et al., 2017;

Qin et al., 2017; Yoon et al., 2002; Zhou et al., 2017). Modes of failures of the rock slope (planar sliding, wedge sliding and flexural toppling) can be identified with its dip/dip direction that contributes to the failure.

2.7 Limit Equilibrium Method (LEM)

Limit Equilibrium Method (LEM) is the most common slope analysis method as it is a relative simple and quick analysis. The data required for analysis can easily be collected from the field (Tang et al., 2017). It is a method based on the assumptions about the slide surface. All points along the slip surface are on verge of failure. LEM will compute Factor of Safety (FoS) where it is a comparison ratio between resisting force and driving force. FoS which is less than one indicates the rock slope is unsafe and failure might occur anytime. Contrarily, FoS which is more than one indicates that the rock slope is safe.

Limit equilibrium method (LEM) is a powerful numerical tool for solving many problems of engineering and mathematical physics. Several limit equilibrium methods (LEM) have been developed for slope stability analysis. Fellenius (1936) introduced the first method, referred to as the Ordinary or the Swedish method, for a circular slip surface. Bishop (1955) advanced the first method introducing a new relationship for the base normal force. The equation for the FoS hence becomes non-linear. At the same time, Janbu N. (1954) developed a simplified method for non-circular failure surfaces, dividing a potential mass into several vertical slices and improved it in Janbu (1973). Later, Morgenstern-Price (1965), Spencer (1967), Sarma (1973) and several others made future contributions with different assumptions for the inter-slice forces. All LEM is based on certain assumptions for the inter-slice normal and shear forces. The comparisons between the methods of slices are presented in Table 2.3.

Table 2.3: Method of slices.

Method	Force Equilibrium		Moment Equilibrium
	Horizontal	Vertical	
Ordinary	No	No	Yes
Bishop Simplified	No	Yes	Yes
Janbu Simplified	Yes	Yes	No
Spencer	Yes	Yes	Yes
Morgenstern-Price	Yes	Yes	Yes
Sarma	Yes	Yes	Yes

Assumptions made in limit equilibrium methods may possibly lead to over simplification. As a result, the results may not be realistic. However, over the years these methods have provided satisfactory results for engineering applications. To have more realistic results on slope stability condition this method can further be integrated with probabilistic methods that can help to recognize and assess uncertainties among the governing parameters in a systematic manner (Alzo'ubi, 2016). Kainthola et al. (2013) used Bishop LEM to conduct probabilistic and sensitivity analysis on the two hill slopes, Chandaak and Chhera in India due to the variability of the parameters of the hills. Besides, locating the critical failure surface of heterogeneous rock slopes is one of the problems which optimization algorithms serve very well to solve them. Bolton et al. (2003) used global optimization algorithm with Janbu's simplified method and Spencer's method to determine the critical failure surface in the slope stability analysis due to the rock having layered profile where the slip surface is complex. No assumptions are required with regards to the geometry of the failure surface and no restrictions are placed on the positions of the initiation and termination point. For homogeneous soils, the assumed failure surface is often of a regular shape and the method of vertical slices in which assumptions about the geometry of the failure surface are made is not suitable. As a result the solution is rendered effectively.